





# Site-Specific Mutations of GalR Affect Galactose Metabolism in *Streptococcus pneumoniae*

Kimberley T. McLean,<sup>a</sup> Alexandra Tikhomirova,<sup>a</sup>  Erin B. Brazel,<sup>a</sup> Salomé Legendre,<sup>a</sup> Gian Haasbroek,<sup>a</sup> Vikrant Minhas,<sup>a</sup>  James C. Paton,<sup>a</sup> Claudia Trappetti<sup>a</sup>

<sup>a</sup>Research Centre for Infectious Diseases, Department of Molecular and Biomedical Science, University of Adelaide, Adelaide, Australia

**ABSTRACT** *Streptococcus pneumoniae* (the pneumococcus) is a formidable human pathogen that is capable of asymptotically colonizing the nasopharynx. Progression from colonization to invasive disease involves adaptation to distinct host niches, which vary markedly in the availability of key nutrients such as sugars. We previously reported that cell-cell signaling via the autoinducer 2 (AI-2)/LuxS quorum-sensing system boosts the capacity of *S. pneumoniae* to utilize galactose as a carbon source by upregulation of the Leloir pathway. This resulted in increased capsular polysaccharide production and a hypervirulent phenotype. We hypothesized that this effect was mediated by phosphorylation of GalR, the transcriptional activator of the Leloir pathway. GalR is known to possess three putative phosphorylation sites, S317, T319, and T323. In the present study, derivatives of *S. pneumoniae* D39 with putative phosphorylation-blocking alanine substitution mutations at each of these GalR sites (singly or in combination) were constructed. Growth assays and transcriptional analyses revealed complex phenotypes for these GalR mutants, with impacts on the regulation of both the Leloir and tagatose 6-phosphate pathways. The alanine substitution mutations significantly reduced the capacity of pneumococci to colonize the nasopharynx, middle ear, and lungs in a murine intranasal challenge model.

**IMPORTANCE** Pneumococcal survival in the host and capacity to transition from a commensal to a pathogenic lifestyle are closely linked to the organism's ability to utilize specific nutrients in distinct niches. Galactose is a major carbon source for pneumococci in the upper respiratory tract. We have shown that both the Leloir and tagatose 6-phosphate pathways are necessary for pneumococcal growth in galactose and demonstrated GalR-mediated interplay between the two pathways. Moreover, the three putative phosphorylation sites in the transcriptional regulator GalR play a critical role in galactose metabolism and are important for pneumococcal colonization of the nasopharynx, middle ear, and lungs.

**KEYWORDS** GalR, *Streptococcus pneumoniae*, carbon metabolism, galactose, pneumococcus, protein phosphorylation, virulence

*Streptococcus pneumoniae* is a human-adapted bacterium often carried asymptotically in the nasopharynx. However, in a proportion of carriers, it can spread to other sites of the body and cause a wide range of illnesses, including otitis media and sinusitis, as well as severe diseases such as bacteremia, pneumonia, and meningitis (1, 2). Globally, *S. pneumoniae* infections account for 1 million to 2 million deaths every year, making it one of the world's foremost bacterial pathogens (3, 4). Colonization of the upper respiratory tract (URT) is an essential prerequisite for invasive disease. However, in this environment, carbon sources are scarce and the host actively eliminates glucose (Glc) to help maintain airway sterility (5). Galactose (Gal) is the most

**Citation** McLean KT, Tikhomirova A, Brazel EB, Legendre S, Haasbroek G, Minhas V, Paton JC, Trappetti C. 2021. Site-specific mutations of GalR affect galactose metabolism in *Streptococcus pneumoniae*. *J Bacteriol* 203: e00180-20. <https://doi.org/10.1128/JB.00180-20>.

**Editor** Ann M. Stock, Rutgers University-Robert Wood Johnson Medical School

**Copyright** © 2020 American Society for Microbiology. All Rights Reserved.

Address correspondence to James C. Paton, [james.paton@adelaide.edu.au](mailto:james.paton@adelaide.edu.au), or Claudia Trappetti, [claudia.trappetti@adelaide.edu.au](mailto:claudia.trappetti@adelaide.edu.au).

**Received** 1 April 2020

**Accepted** 2 October 2020

**Accepted manuscript posted online** 12 October 2020

**Published** 7 December 2020

abundant sugar in the URT (6), so it follows that the ability to metabolize it may be a crucial factor for pneumococcal survival within host niches.

In a previous study, we discovered a direct link between carbohydrate utilization and virulence (7). In particular, we found that the quorum-sensing signaling molecule autoinducer 2 (AI-2) promotes transition of the pneumococcus from colonizer to pathogen. Importantly, AI-2 signaling via the fructose-specific phosphoenolpyruvate phosphotransferase system (PTS) component FruA enables the bacterium to utilize Gal as a carbon source and upregulates the Leloir pathway, thereby leading to increased production of capsular polysaccharide (CPS) and a hypervirulent phenotype (7). CPS precursors are synthesized from Glc 1-phosphate, which can be produced via either the Glc 6-phosphate pathway in the presence of Glc (as occurs in the blood) or the Leloir pathway when Gal is the predominant sugar (as occurs in the URT).

*S. pneumoniae* possesses two pathways for galactose metabolism, the Leloir pathway and the tagatose 6-phosphate (T6P) pathway. In the T6P pathway, extracellular Gal is transported into the cell and phosphorylated through a PTS (unrelated to FruA) (8). The resultant Gal 6-phosphate is then converted into T6P by the enzyme Gal 6-phosphate isomerase (encoded by *lacAB*). The T6P kinase (encoded by *lacC*) then converts T6P into tagatose 1,6-bP. Finally, *lacD* codes for the tagatose 1,6-bP aldolase, which converts tagatose 1,6-bP into dihydroxyacetone-P and D-glyceraldehyde-3-P (9, 10). In the Leloir pathway, Gal enters the cell via a proposed ABC transporter (8). It is then phosphorylated intracellularly at the C1 position by a specific kinase (encoded by *galk*) to yield Gal 1-phosphate, which is then converted into Glc 1-phosphate by hexose 1-phosphate uridylyltransferase (encoded by *galT*) and UDP-glucose epimerase (encoded by *galE*). The transcriptional regulator of this pathway is GalR, which is believed to possess three putative phosphorylation sites, S317, T319, and T323 (11). We previously proposed that phosphorylated AI-2 imported via FruA facilitates phosphorylation of GalR at these sites, thereby activating (or relieving repression of) the *gal* operon (7). In the present study, we conducted mutational analysis of the putative GalR phosphorylation sites and examined the impact on expression of Leloir and T6P pathway genes and Gal metabolism.

## RESULTS

**The location of the GalR putative phosphorylation sites.** In the absence of structural information for GalR, we sought to examine the location of the putative phosphorylated residues (S317, T319, and T323) by generating a structural homology model. A homology model of GalR was constructed using SWISS-MODEL based on the homodimeric 2.4-Å structure (PDB: 1JFS) of the *Escherichia coli* PurR W147F mutant (35% sequence similarity, 93% sequence coverage) (12). Alignment of the GalR model (green) with the template (cyan) revealed a moderate level of variation (root mean square deviation [RMSD], 2.868 Å), with an additional loop present in the GalR model that was absent in PurR, corresponding to residues 183 to 191 (Fig. 1A). To complement these studies, we performed a conserved domain search to investigate whether any of the putative phosphorylated residues were located within regions of possible functional importance (Fig. 1B). The putative galactose binding residues (magenta) are situated at the putative dimer interface of GalR, suggesting a role in protein dimer stabilization upon sugar binding, while the N-terminal region of GalR harbors the helix-turn-helix domain (blue) responsible for the interaction with DNA. All of the putative phosphorylated residues (orange spheres) were situated in a region distinct from the residues proposed to be involved in galactose binding and DNA binding (Fig. 1B). As any functional impact of S317, T319, or T323 phosphorylation is more likely a consequence of allosteric changes rather than a direct impact on sugar or DNA binding, we investigated the contribution of each putative phosphorylated residue to GalR function. We constructed a series of GalR amino acid substitution mutants in *S. pneumoniae* D39 in which S317, T319, and T323 were replaced, either singly or in combination, with the nonphosphorylatable residue alanine (A), using the Janus cassette system (see Materials and Methods). A total of 7 substitution mutants were

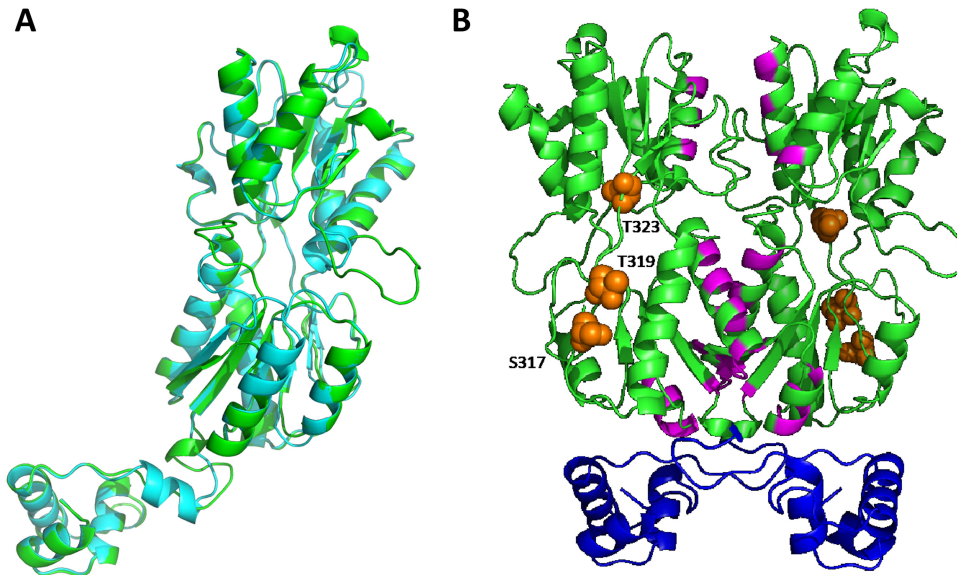


**FIG 1** Structural homology model of *S. pneumoniae* GalR. (A) Cartoon representation of the protomeric homology model of *S. pneumoniae* GalR (green) based on the 2.9-Å structure of the *Escherichia coli* PurR W147F mutant (cyan; RMSD, 2.868 Å). (B) Cartoon representation of the dimeric homology model of GalR. The DNA binding helix-turn-helix domain is shown in blue, and the putative sugar binding regions are highlighted in magenta. The serine (S317) and threonine (T319 and T323) residues hypothesized to be phosphorylated are depicted as orange spheres.

generated (designated D39<sub>AAA</sub>, D39<sub>ATT</sub>, D39<sub>SAT</sub>, D39<sub>STA</sub>, D39<sub>AAT</sub>, D39<sub>ATA</sub>, and D39<sub>SAA</sub>), as well as a *galR* deletion mutant (D39Δ*galR*) (see Table 1).

#### Impact of GalR putative phosphorylation sites on galactose metabolism.

Growth in chemically defined medium with Glc as the sole carbon source (CDM + Glc) revealed that each mutant grew comparably to the D39 wild-type strain (Fig. 2A). Conversely, when grown in chemically defined medium with Gal as the sole carbon source (CDM + Gal), significant growth differences between strains became apparent (Fig. 2B). First, in comparison to D39, the D39Δ*galR* strain displayed complete abrogation of growth in the presence of Gal, indicating an essential role for *galR* in the ability to utilize galactose, as previously shown (13). The D39<sub>AAA</sub> strain, where the three putative phosphorylation sites are nonphosphorylatable, showed almost a complete inability to grow in galactose. D39<sub>SAA</sub> showed a delay in growth, with a slower generation time and a decrease in final cell density compared to D39. The remaining GalR substitution mutants, D39<sub>ATT</sub>, D39<sub>SAT</sub>, D39<sub>STA</sub>, D39<sub>AAT</sub>, and D39<sub>ATA</sub>, had a capacity to utilize Gal similar to that of D39. This indicates that mutation of any one of the three

**TABLE 1** Strains used in this study

Strain	Description <sup>a</sup>	Source
D39	Capsular serotype 2	NCTC 7466
D39Δ <i>galR</i>	<i>galR</i> deletion-replacement mutant, erythromycin <sup>r</sup>	This study
D39Δ <i>galK</i>	<i>galK</i> deletion-replacement mutant, spectinomycin <sup>r</sup>	This study
D39Δ <i>lacAB</i>	<i>lacAB</i> deletion-replacement mutant, spectinomycin <sup>r</sup>	This study
D39Δ <i>lacD</i>	<i>lacD</i> deletion-replacement mutant, erythromycin <sup>r</sup>	This study
D39Δ <i>galR</i> Δ <i>lacD</i>	<i>galR</i> , <i>lacD</i> deletion-replacement mutant, erythromycin <sup>r</sup> and spectinomycin <sup>r</sup>	This study
D39Δ <i>galR</i> Janus	<i>galR</i> deletion-replacement mutant utilizing Janus cassette, kanamycin <sup>s</sup> , streptomycin <sup>s</sup>	This study
D39 <sub>AAA</sub>	<i>galR</i> S317A, T319A, T323A amino acid substitution mutant, kanamycin <sup>s</sup> , streptomycin <sup>s</sup>	This study
D39 <sub>ATT</sub>	<i>galR</i> S317A amino acid substitution mutant, kanamycin <sup>s</sup> , streptomycin <sup>r</sup>	This study
D39 <sub>SAT</sub>	<i>galR</i> T319A amino acid substitution mutant, kanamycin <sup>s</sup> , streptomycin <sup>r</sup>	This study
D39 <sub>STA</sub>	<i>galR</i> T323A amino acid substitution mutant, kanamycin <sup>s</sup> , streptomycin <sup>r</sup>	This study
D39 <sub>AAT</sub>	<i>galR</i> S317A, T319A amino acid substitution mutant, kanamycin <sup>s</sup> , streptomycin <sup>r</sup>	This study
D39 <sub>ATA</sub>	<i>galR</i> S317A, T323A amino acid substitution mutant, kanamycin <sup>s</sup> , streptomycin <sup>r</sup>	This study
D39 <sub>SAA</sub>	<i>galR</i> T319A, T323A amino acid substitution mutant, kanamycin <sup>s</sup> , streptomycin <sup>r</sup>	This study

<sup>a</sup>Superscript "r" and "s" following antibiotic names indicate resistance and sensitivity, respectively.

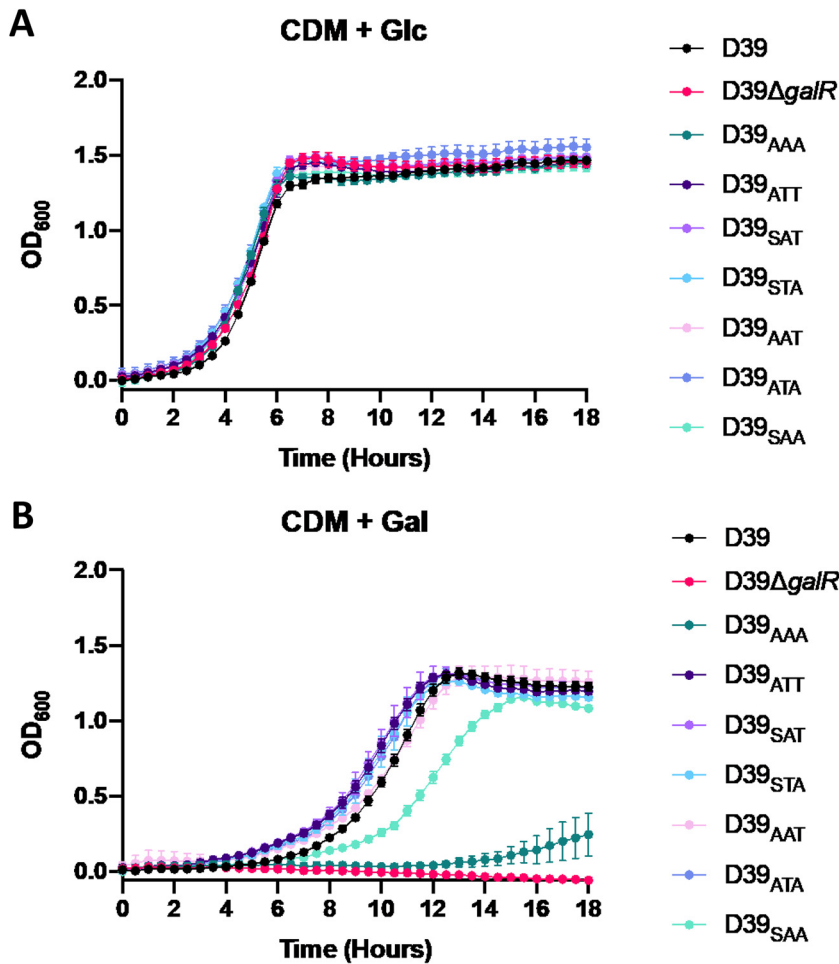


**FIG 2** Impact of GalR mutations on bacterial growth. D39, D39 $\Delta galR$ , D39<sub>AAA</sub>, D39<sub>ATT</sub>, D39<sub>SAT</sub>, D39<sub>STA</sub>, D39<sub>AAT</sub>, D39<sub>ATA</sub>, and D39<sub>SAA</sub> were grown in CDM + Glc (A) or CDM + Gal (B). Growth was monitored by measuring the OD<sub>600</sub> every 30 min for a total of 18 h. Data points are the mean OD<sub>600</sub> from triplicate assays.

GalR phosphorylation sites alone does not significantly impact the capacity to grow in CDM + Gal. However, mutation of both T319 and T323, as occurs in D39<sub>SAA</sub>, reduced the capacity of the strain to grow in this medium. Thus, the first GalR phosphorylation site (S317) on its own is insufficient to fully sustain growth in Gal.

To complement these data, gene expression analyses were conducted on all the GalR mutants to assess the impact on expression of both Leloir and T6P pathway genes. Strains were grown overnight on blood agar, washed and resuspended in CDM + Gal, and then incubated for 30 min. RNA was then extracted, and expression of *galR*, *galk*, and *lacD* was quantitated by reverse transcription-qualitative PCR (qRT-PCR) (see Materials and Methods) (Fig. 3). Expression of *galR* itself was, as expected, undetectable in D39 $\Delta galR$ . *galR* expression was also significantly downregulated in all the mutants tested, with D39<sub>AAA</sub> being the most affected, showing an 88% reduction in expression (Fig. 3A).

It was previously shown that *galR* regulates the *galkT* operon (14). Here, there was significantly decreased expression of *galk* in all GalR mutants compared to wild-type D39 (Fig. 3B). In particular, the D39 $\Delta galR$  and D39<sub>AAA</sub> strains showed similarly low levels of *galk* expression ( $\geq 98\%$  reduction). These findings are largely consistent with the effects of the mutations on the expression of *galR* itself (Fig. 3A). It is worth noting that only those mutants with  $>98\%$  reduction in *galk* expression (D39 $\Delta galR$  and D39<sub>AAA</sub>) exhibited severe growth defects in CDM + Gal (Fig. 2B).

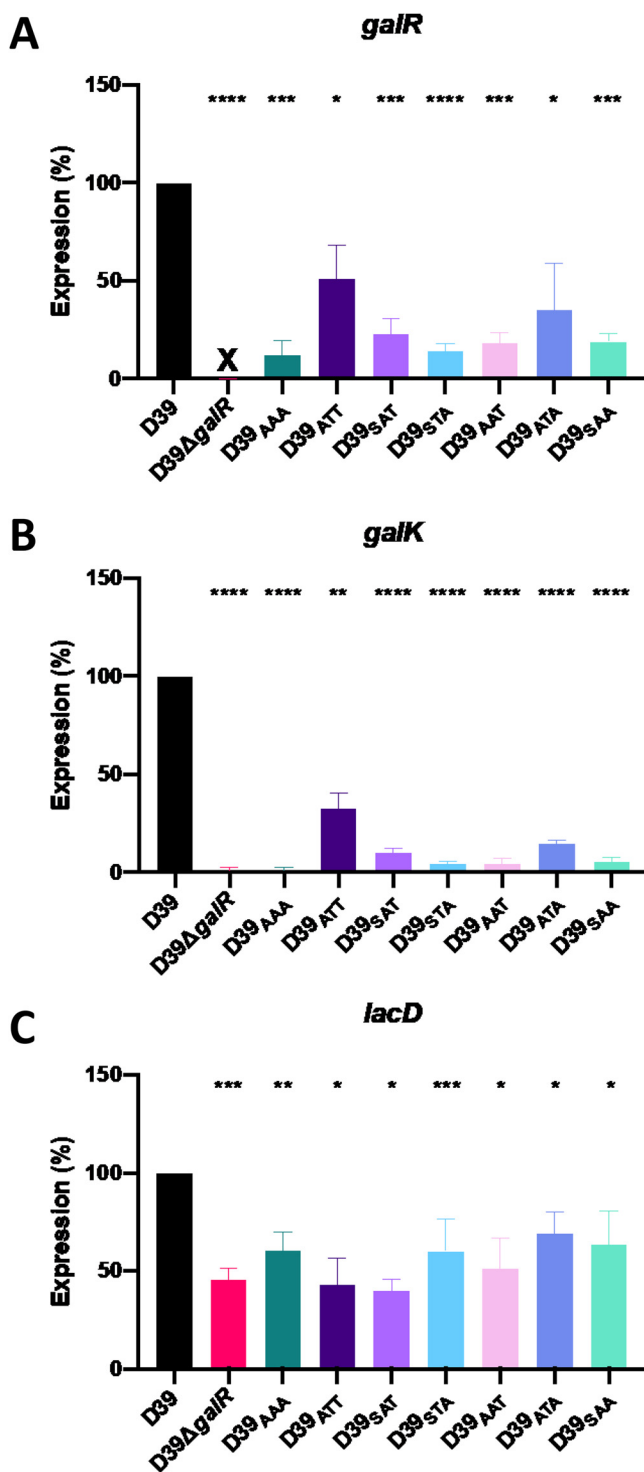


**FIG 3** Differential gene expression in GalR mutants. D39, D39Δ*galR*, D39<sup>AAA</sup>, D39<sup>ATT</sup>, D39<sup>sAT</sup>, D39<sup>sTA</sup>, D39<sup>AAT</sup>, D39<sup>ATA</sup>, and D39<sup>sAA</sup> were cultured overnight on blood agar plates, washed, and resuspended to a final OD<sub>600</sub> of 0.25 in CDM + Gal and incubated for 30 min. RNA was then extracted and the levels of *galR* (A), *galK* (B), and *lacD* (C) mRNA were quantitated by qRT-PCR using *gyrA* as an internal control. Data presented are the mean ± standard deviation from three independent experiments, expressed as a percentage of the result for D39. \*,  $P < 0.05$ ; \*\*,  $P < 0.01$ ; \*\*\*,  $P < 0.001$ ; \*\*\*\*,  $P < 0.0001$ , unpaired  $t$  test (relative to D39); ns, not significant; X, transcript absent due to gene deletion.

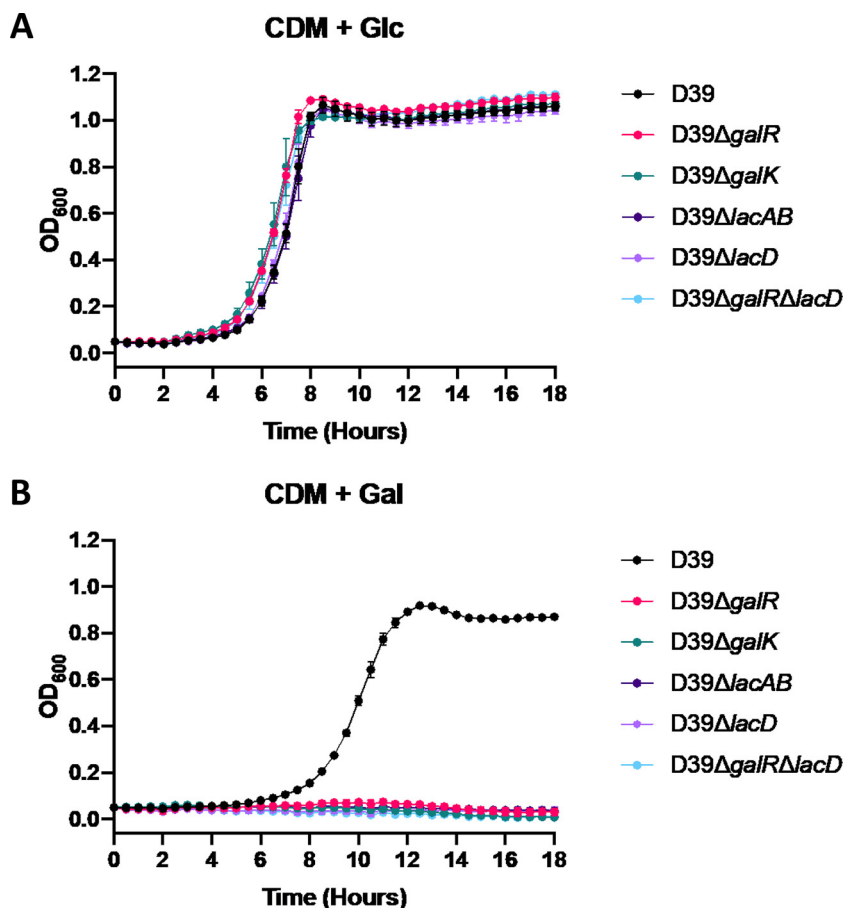


**FIG 4** Differential growth of Leloir and T6P pathway mutants. D39, D39Δ*galR*, D39Δ*galk*, D39Δ*lacAB*, D39Δ*lacD*, and D39Δ*galRΔlacD* were grown in CDM + Glc (A) or CDM + Gal (B). Growth was monitored by measuring the OD<sub>600</sub> every 30 min for 18 h. Data points are the mean OD<sub>600</sub> from triplicate assays.

We also assessed whether the absence of functional Leloir pathway expression had any effect on the expression of the T6P pathway by examining *lacD* expression. *lacD* encodes the last enzyme of the T6P pathway and is responsible for the conversion of tagatose 1,6-bP to dihydroxyacetone-P and D-glyceraldehyde-3-P, which can then feed into the glycolytic pathway. Interestingly, *lacD* expression was significantly (30 to 60%) lower in all GalR mutants than in D39 (Fig. 3C), indicating a direct or indirect role for GalR phosphorylation in the expression of T6P pathway genes. However, there was no apparent association between reduced *lacD* expression and the relative ability of the various strains to grow in CDM + Gal (Fig. 2B). Collectively, these analyses indicate that all three putative GalR phosphorylation sites, S317, T319, and T323, are essential for galactose metabolism in *S. pneumoniae* and are required for the activation of both the Leloir and T6P pathways.

**Both the Leloir and T6P pathways are required for growth in galactose.** In order to assess the contribution of the Leloir and T6P pathways to Gal metabolism, growth of D39, D39Δ*galR*, D39Δ*galk*, D39Δ*lacAB*, D39Δ*lacD*, and D39Δ*galRΔlacD* was analyzed in both CDM + Glc and CDM + Gal (Fig. 4). All mutant strains grew as well as D39 when Glc was the only carbon source (Fig. 4A). In contrast, in CDM + Gal, all mutant strains displayed complete abrogation of growth (Fig. 4B). Thus, the presence of both the functional Leloir and T6P pathways is required for growth in Gal, indicating potential interplay between these two pathways.

**Contribution of GalR and its putative phosphorylation sites to regulation of Gal metabolism.** To further understand the apparent cross talk between the Leloir and T6P pathways, we analyzed the expression of *galR*, *galk*, *lacA*, and *lacD* in D39,

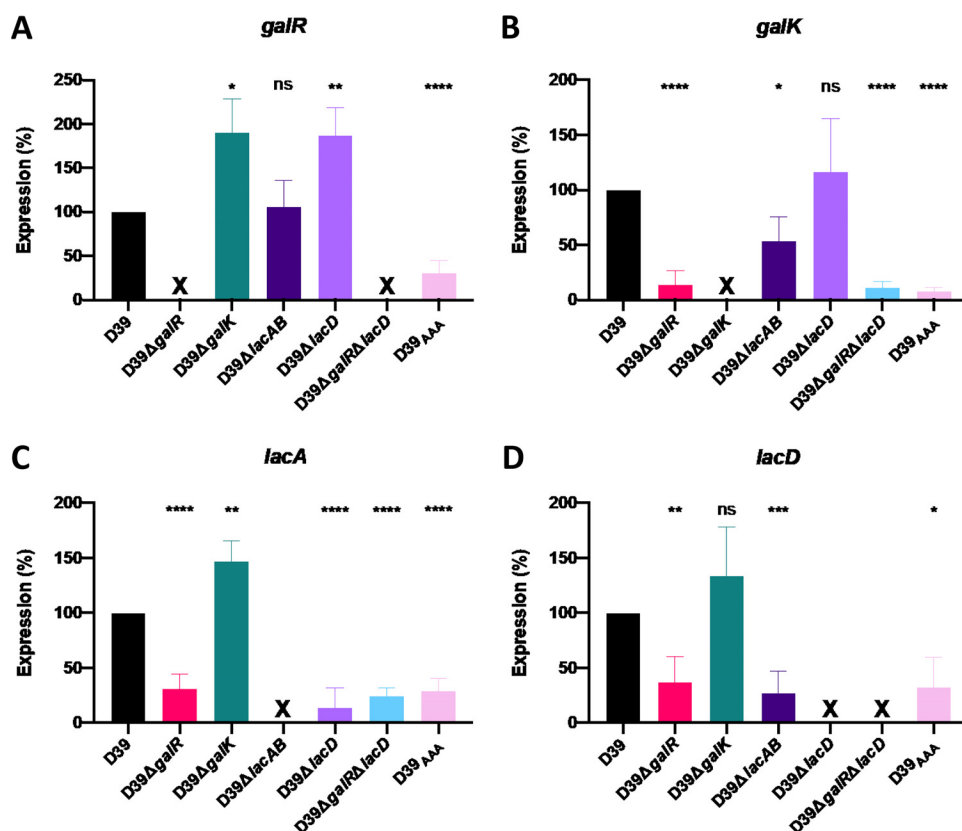


**FIG 5** Differential gene expression in Leloir and T6P pathway mutants. D39, D39ΔgalR, D39ΔgalK, D39ΔlacAB, D39ΔlacD, D39ΔgalRΔlacD, and D39<sub>AAA</sub> were cultured overnight on blood agar, washed, and resuspended to a final OD<sub>600</sub> of 0.25 in CDM + Gal and incubated for 30 min. RNA was then extracted, and qRT-PCR was used to assess levels of *galR*, *galK*, *lacAB*, and *lacD* mRNA, using *gyrA* as an internal control. Data presented are the mean ± standard deviation from three independent experiments, expressed as a percentage of that for D39. \*,  $P < 0.05$ ; \*\*,  $P < 0.01$ ; \*\*\*,  $P < 0.001$ ; \*\*\*\*,  $P < 0.0001$ , by unpaired *t* test (relative to D39); ns, not significant; X, transcript absent due to gene deletion.

D39ΔgalR, D39ΔgalK, D39ΔlacAB, D39ΔlacD, D39ΔgalRΔlacD, and D39<sub>AAA</sub> (Fig. 5). The expression of *galR* was significantly upregulated in both D39ΔgalK and D39ΔlacD relative to D39, whereas it was unaffected in D39ΔlacAB (Fig. 5A). *galK* expression was unaffected in D39ΔlacD but was significantly downregulated relative to D39 in D39ΔlacAB (Fig. 5B). Both *galR* and *galK* expression were also largely abrogated in D39ΔgalR and D39<sub>AAA</sub>, confirming the requirement for functional GalR for activation of the Leloir pathway, as previously shown in Fig. 3B. Unsurprisingly, the expression of these two genes was also abrogated in D39ΔgalRΔlacD.

Interestingly, *lacA* expression (Fig. 5C) was significantly upregulated relative to D39 in D39ΔgalK. In the remaining mutants, the expression of both *lacA* and *lacD* was downregulated relative to D39 (Fig. 5C and D). Collectively, these findings underscore the requirement for GalR (and putative phosphorylation sites therein) for upregulation of the T6P pathway when the Leloir pathway is blocked. This could be due to feedback inhibition from accumulation of either Leloir or T6P intermediates. We also assessed expression of *lacR2*, the repressor of the *lacI* operon. In the presence of Gal, there was a significant decrease in expression of *lacR2* in D39ΔlacD relative to D39, implying derepression of the operon to promote upregulation of the T6P pathway genes. However, there was no significant difference in *lacR2* expression between D39 and D39ΔgalR, indicating that effects of GalR on T6P pathway gene expression are not mediated via *lacR2* (data not shown).

**Impact of putative GalR phosphorylation in a mouse model of pneumococcal infection.** To determine the role of putative GalR phosphorylation during pneumococ-

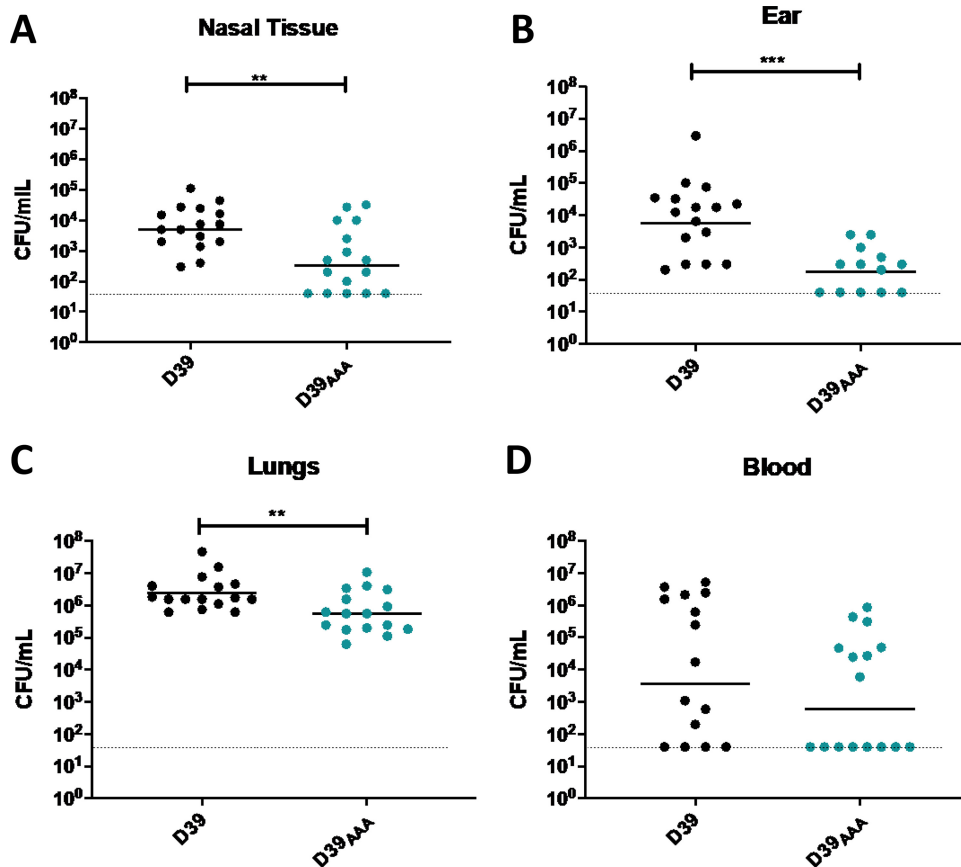


**FIG 6** Virulence phenotypes of D39 and D39<sub>AAA</sub>. Groups of 16 mice were infected intranasally with  $10^7$  CFU of the indicated strain. At 24 h, mice were euthanized, and the numbers of pneumococci isolated from the nasal tissue (A), ears (B), lungs (C), and blood (D) were enumerated. Viable counts (total CFU per tissue or CFU per ml blood) are shown for each mouse in each niche; the horizontal bars indicate the geometric mean (GM) CFU for each group; the dotted line indicates the threshold of detection. The significance of the differences in GM bacterial load between groups was analyzed using unpaired *t* tests; \*,  $P < 0.05$ ; \*\*,  $P < 0.01$ ; \*\*\*,  $P < 0.001$ .

cal infection, the virulence of the *S. pneumoniae* D39 and D39<sub>AAA</sub> strains was assessed in a murine model of infection. Groups of mice were challenged intranasally with  $1 \times 10^7$  CFU of each strain, and the numbers of pneumococci present in various niches (nasal tissue, ear, lungs, and blood) were determined at 24 h postchallenge (Fig. 6). The D39<sub>AAA</sub> strain exhibited a significantly attenuated virulence phenotype, with reduced bacterial loads relative to D39 in nasal tissue (Fig. 6A), ears (Fig. 6B), and lungs (Fig. 6C). No significant difference in bacterial numbers between D39 and D39<sub>AAA</sub> was observed in the blood (Fig. 6D).

## DISCUSSION

The results of this study support previous findings that GalR is important for galactose metabolism in *S. pneumoniae* (14). Here, we demonstrated that the putative GalR phosphorylation sites (S317, T319, and T323) are required for growth in a defined medium with Gal as the sole carbon source. Mutation of all putative phosphorylation sites to alanine (D39<sub>AAA</sub>) completely abrogated growth in Gal and reduced expression of *galR* and *galK* to levels comparable to those of the D39 $\Delta$ *galR* strain (Fig. 2B and Fig. 3). Moreover, the substitution of these amino acids with alanine appears to alter the interaction of GalR with the *galR* operator sequence; as a result, the defects observed in *galK* expression may be at least partially attributable to a reduction in GalR abundance, rather than a direct alteration in binding to the *galK* operator. The precise mechanism behind these defects remains unknown but may be due to effects on folding, dimerization, or binding of effector molecules rather than by directly prevent-



ing phosphorylation. However, structural modeling of GalR shows that these residues are positioned in a distinct location to the putative galactose and DNA binding regions (Fig. 1B). Additional studies exploring the interaction of purified GalR and GalR<sub>AAA</sub> with each operator DNA sequence may provide greater insight into the regulation of the Leloir pathway genes.

In *S. pneumoniae*, the kinase responsible for phosphorylation of serine and threonine residues is StkP (15, 16). A previous proteomic study performed in medium containing Glc failed to identify GalR as a target of StkP, but LacA was identified as a possible target for StkP-mediated phosphorylation (17). Preliminary data have revealed that a D39 $\Delta$ stkP strain was unable to grow in Gal (data not shown), but this may be a consequence of the defect in LacA phosphorylation rather than GalR. As a result, additional studies to directly examine the role of StkP in GalR phosphorylation are required.

Gene expression studies demonstrated that of the various GalR mutants constructed in this study, those with the greatest defects in growth in CDM + Gal, namely, D39 $\Delta$ galR and D39<sub>AAA</sub>, exhibited virtually undetectable levels of *galK* expression (>98% reduction) (Fig. 3B), showing a direct link between Leloir pathway gene expression and growth in Gal. The single and double point mutants also showed significantly reduced expression of *galR* and *galK*, but this level of expression still enabled sufficient Leloir pathway activity to sustain growth in CDM + Gal (Fig. 2B). Interestingly, within the single or double point mutants, the D39<sub>SAA</sub> mutant was the only one to show a defect in growth in Gal compared to D39 (Fig. 2B), but gene expression was similar to that in the other mutants that grew comparably to the wild type (Fig. 2B and Fig. 3). Therefore, growth in Gal can occur even at low levels of *galK* expression. Thus, the effects on Leloir pathway gene expression and growth in CDM + Gal could be attributable to inadequate levels of GalR in the cell, reduced capacity of the respective GalR phosphorylation site mutants to activate Leloir pathway genes such as *galK*, or a combination of both.

An unexpected finding of the current study was that all the investigated GalR mutants exhibited significantly reduced expression of the T6P pathway gene *lacD* (Fig. 3C), indicating a direct or indirect effect of GalR on the T6P pathway. This may provide a mechanistic basis for a previously proposed subtle regulatory link between the Leloir and T6P pathways (6). This was further examined by comparing the growth and gene expression phenotypes of D39 mutants with deletions in *galR*, *galK*, *lacAB*, *lacD*, and *galR* plus *lacD*. Unlike growth in CDM + Glc, none of these mutants was capable of growth in CDM + Gal (Fig. 4), indicating that both the Leloir and T6P pathways are essential for growth under these conditions. A previous study of a similar D39 *galK* deletion mutant (14) reported that growth in the presence of Gal was reduced relative to wild-type D39 but not completely abrogated as shown in the present study. This discrepancy may be attributable to the use of a more nutrient-rich M17 medium in that study (14). A separate study reported complete abrogation of growth of a D39 *galK* deletion mutant in Gal, whereas a *lacD* deletion mutant was able to grow logarithmically in Gal, albeit after a long lag phase (6).

In the present study, gene expression analyses have shown that maximal expression of the T6P pathway genes *lacA* and *lacD* require functional GalR and that all three putative phosphorylation sites of GalR are necessary to achieve this function (Fig. 5). Additionally, there appears to be a link between *galK* and *lacAB* gene expression. Deletion of *galK* upregulated *lacA* expression, perhaps as a consequence of the upregulation of *galR* in this mutant. On the other hand, deletion of *lacAB* significantly reduced *galK* expression but did not impact expression of *galR*. Furthermore, *galR* expression was significantly elevated in the *lacD* mutant. Thus, there is a complex interplay between the Leloir and T6P pathways in the various mutants, presumably mediated by intracellular concentrations of intermediates or end products of either pathway.

Notwithstanding the above-described complexities, the present study has shown that the GalR putative phosphorylation sites play a significant role in pneumococcal infection. Mice infected with D39<sub>AAA</sub> displayed significantly reduced bacterial loads in

the nasopharynx, middle ear, and lungs relative to those infected with wild-type D39 (Fig. 6). These findings are compatible with previous studies showing reduced nasopharyngeal colonization and reduced systemic virulence of D39 *galK* and *lacD* deletion mutants after intranasal, but not intravenous, challenge of mice (6). However, the impact of the putative GalR phosphorylation sites has not previously been investigated. Clearly, the capacity to metabolize Gal is important for survival and proliferation in the upper respiratory tract and the middle ear, where it is an important carbon source (6). Moreover, metabolism of Gal by pneumococci *in vitro* is known to lead to increased production of CPS relative to cells growing on Glc, which may be the basis for the altered virulence profiles (7). We previously showed that treatment with the quorum-sensing molecule AI-2 upregulates Leloir pathway gene expression and CPS production in the presence of Gal *in vitro*, as well as virulence in an intranasal challenge model (7). This upregulation was dependent on the PTS component FruA, which is presumed to be the bacterial surface receptor for AI-2. This signaling molecule is a di-ketopentose and may structurally mimic the natural cargo of FruA, namely, fructose, and if AI-2 is capable of internalization via the FruA PTS system, then it would be expected to be phosphorylated during import. It is tempting to speculate that such phosphorylated AI-2 may play a direct or indirect role in GalR phosphorylation, perhaps acting as a phosphate donor, thereby mediating upregulation of the Leloir pathway. This study has shown that, collectively, the GalR putative phosphorylation sites play a key role in virulence and the ability to metabolize Gal and has revealed a complex interplay between the Gal metabolic pathways in *S. pneumoniae*.

## MATERIALS AND METHODS

**Structural modeling of GalR.** The GalR amino acid sequence (SPD\_1635) was obtained from the NCBI database and input into SWISS-MODEL (18). A homology model was generated based on the 2.4-Å structure (PDB: 1JFS) of the *Escherichia coli* purine repressor (PurR) W147F mutant (12). The cartoon representation of the GalR homology model and the aligned PurR template were generated in PyMOL version 2.3.3 (Schrödinger). The root mean square deviation (RMSD) between the GalR model and the PurR template was determined by alignment in PyMOL. The DNA binding domain and putative sugar binding residues were identified by the NCBI conserved domain search (19), and the locations of the putative phosphorylated residues were determined based on the phosphoproteomic findings (11).

**Bacterial strains and growth conditions.** The *S. pneumoniae* strains used in this study are listed in Table 1. Pneumococci were routinely cultured on Columbia blood agar base supplemented with 5% sterile horse blood overnight at 37°C with 5% CO<sub>2</sub>. In order to select for mutant strains, blood agar plates were supplemented with 0.2 μg/ml erythromycin, 200 μg/ml spectinomycin, 200 μg/ml kanamycin, or 200 μg/ml streptomycin, as appropriate. Growth experiments were performed with pneumococci grown in chemically defined medium (CDM) supplemented with vitamins, amino acids, choline, and catalase, as previously described (20), and either 0.5% glucose (CDM + Glc) or galactose (CDM + Gal).

**Construction of mutants.** Genes were deleted from *S. pneumoniae* using overlap PCR using the primers listed in Table 2, followed by transformation, essentially as previously described (21). For strains harboring single amino acid substitutions within *galR*, allelic exchange mutagenesis was performed through use of the Janus cassette system, as described previously (20, 22). Mutants were confirmed by PCR and Sanger sequencing using the primers listed in Table 2 (AGRF, Adelaide, Australia).

**Growth assays.** Growth assays were performed in flat-bottom 96-well microtiter plates with a final volume of 200 μl. Cells were inoculated at a starting optical density at 600 nm (OD<sub>600</sub>) of 0.05 in either CDM + Glc or CDM + Gal and then incubated at 37°C with 5% CO<sub>2</sub> (20). The OD<sub>600</sub> was measured every 30 min for a total of 18 h in a SpectroSTAR Omega spectrophotometer (BMG Labtech). Assays were performed in triplicate with a minimum of two independent experiments.

**Bacterial RNA extraction and real-time qRT-PCR.** *S. pneumoniae* strains were first cultured overnight on blood agar plates at 37°C with 5% CO<sub>2</sub>. Cells were then harvested, washed, and resuspended in 1 ml of CDM + Gal to a final OD<sub>600</sub> of 0.25. Cells were then incubated for 30 min at 37°C with 5% CO<sub>2</sub>, after which RNA was extracted using a Qiagen RNeasy minikit as per the manufacturer's instructions. Gene expression was analyzed using one-step relative real-time qRT-PCR in a Roche LC480 real-time cyclor, as described previously (20). The primers used to amplify target genes (listed in Table 2) were used at a final concentration of 200 nM. Amplification data were analyzed using the comparative critical threshold (2<sup>ΔΔCT</sup>) method (23) and are presented as a percentage of total expression relative to that for D39 for each gene. Assays were performed in triplicate with a minimum of two independent experiments. Statistical analyses were performed using two-tailed Student's *t* test; *P* values of <0.05 were deemed statistically significant.

**Murine infection model.** All animal experiments were approved by the University of Adelaide Animal Ethics Committee. Female outbred 4- to 6-week-old CD-1 (Swiss) mice were anaesthetized by intraperitoneal injection with ketamine and xylazine before being intranasally inoculated with 1 × 10<sup>7</sup> CFU of D39 or D39<sub>AAA</sub> in a total of 50 μl, as previously described (24). The challenge dose was

**TABLE 2** Primers used in this study

Primer	Sequence (5'–3')
GalR F	AAGACAAGCCAGAACCATTGGG
GalR Ery F	CGGGAGGAAATAATTCTATGAGGAAAGTACCCTAAATCAAGAATAG
GalR R	GACAAGGTTGTTGTTATCGGTGAT
GalR Ery R	TTGTTTCATGTAATCACTCCTTCTGTGCAATGTCTTTTAAGGTAGCC
LacD F	CTGTATCGCTATTCTCCACG
LacD Ery F	CGGGAGGAAATAATTCTATGAGGGTATCATCTCAGCTCTTGC
LacD R	TGATCTGCTAGCTTCTGAC
LacD Ery R	TTGTTTCATGTAATCACTCCTTCGCAAGAGCTGAGATGATACC
Ery F	GAAGGAGTGATTACATGAACAA
Ery R	CTCATAGAATTATTCTCCCG
GalK F	CCTTCATTAAGTCATAGCCAGA
GalK Spec F	AAATAACAGATTGAAGAAGGTATAAGAAGTAGTTGGATACGCTCC
GalK R	GTAGGACAGACATTGGCCA
GalK Spec R	TATGTATTCATATATATCCTCCTCCAAATTGATACGACCTGGTG
LacAB F	AATATCGGACAAGCTGGT
LacAB Spec F	AAATAACAGATTGAAGAAGGTATAAGCTCAACAAACAGACGC
LacAB R	TTCGTCTGAGCTATCTACATC
LacAB Spec R	TATGTATTCATATATATCCTCCTCATCTCAAACCTGCAGCATC
LacD F	CTGTATCGCTATTCTCCACG
LacD Spec F	AAATAACAGATTGAAGAAGGTATAATGAAGCAGCAGCTCGCGAAT
LacD R	TATGTATTCATATATATCCTCCTCGCAAGAGCTGAGATGATACC
LacD Spec R	GTTGCGTAATCACATCATAGAT
J253	GAGGAGGATATATGAATACATACG
J254	TTATACCTTCTCAATCTGTTATTTAAATAGTTTATAGTTA
AAA F	ACTCCACGGTCGCAAAATTCCTGCGCTGGCCATGCTGGGAGCCAGACTGACATTAAGA
AAA R	TCTTAATGTCAGTCTGGCTCCCAGCATGGCCAGCGCAGGAATTTTGCACCGTGGAGT
ATT F	AGTACTCCACGGTCGCAAAATTCCTGCCCCTGACCATGCTGGGAACCAGACTGACATTAAGAGAAAAGTACCC
ATT R	GGGTACTTTTCTTAATGTCAGTCTGGTCCCAGCATGGTCAGGGCAGGAATTTTGCACCGTGGAGTACT
SAT F	AGTACTCCACGGTCGCAAAATTCCTAGCCTGGCCATGCTGGGAACCAGACTGACATTAAGAGAAAAGTACCC
SAT R	GGGTACTTTTCTTAATGTCAGTCTGGTCCCAGCATGGCCAGGCTAGGAATTTTGCACCGTGGAGTACT
STA F	AGTACTCCACGGTCGCAAAATTCCTAGCCTGACCATGCTGGGAGCCAGACTGACATTAAGAGAAAAGTACCC
STA R	GGGTACTTTTCTTAATGTCAGTCTGGTCCCAGCATGGTCAGGCTAGGAATTTTGCACCGTGGAGTACT
AAT F	AGTACTCCACGGTCGCAAAATTCCTGCCCCTGGCCATGCTGGGAACCAGACTGACATTAAGAGAAAAGTACCC
AAT R	GGGTACTTTTCTTAATGTCAGTCTGGTCCCAGCATGGCCAGGGCAGGAATTTTGCACCGTGGAGTACT
ATA F	AGTACTCCACGGTCGCAAAATTCCTGCCCCTGACCATGCTGGGAGCCAGACTGACATTAAGAGAAAAGTACCC
ATA R	GGGTACTTTTCTTAATGTCAGTCTGGTCCCAGCATGGTCAGGGCAGGAATTTTGCACCGTGGAGTACT
SAA R	AGTACTCCACGGTCGCAAAATTCCTAGCCTGGCCATGCTGGGAGCCAGACTGACATTAAGAGAAAAGTACCC
SAA R	GGGTACTTTTCTTAATGTCAGTCTGGTCCCAGCATGGCCAGGCTAGGAATTTTGCACCGTGGAGTACT
gyr-RT-F	ACTGGTATCGCGGTTGGGAT
gyr-RT-R	ACCTGATTTTCCCATGCAA
galR-RT-F	TCTCTATCGCCGACCGTATCC
galR-RT-R	GGGTAGCCCAGCTCTTCAG
galK-RT-F	CACGTTTCTCTGGAGCATGA
galK-RT-R	ATGGCACAGCCACTAAAACC
galT-RT-F	GTGGGAGAAGGTGTTTTGGA
galT-RT-R	ACGCGCAGTCTGACTATCCT
lacA-RT-F	CGTGATTGATGCTTATGGAG
lacA-RT-R	AGCCAATTCATCACCACAAG
lacD-RT-F	CATCGGTTCTGAGTGTGTTG
lacD-RT-R	AAAGCGTGGGCTGAAAAGA
galR-Seq F	AATCTATCATGATGAACTGGTC
galR-Seq R	CATAATGGAGGGCGTATGG

retrospectively confirmed by serial dilution and plating on blood agar plates. At 24 h postinfection, mice were euthanized by CO<sub>2</sub> asphyxiation before harvesting the blood, lungs, nasal tissue, and ears. Pneumococci were enumerated from homogenized tissue as described previously by serial dilution and plating on Columbia blood agar plates supplemented with 40 µg/ml gentamicin (20). Statistical analyses of log-transformed CFU data were performed using two-tailed Student's *t* test; *P* values of <0.05 were deemed statistically significant.

## ACKNOWLEDGMENTS

We acknowledge the contributions of Patrick R. Andreassen, Shannon C. David, and Hannah N. Agnew for assistance with mutant generation and animal experiments.

This work was supported by the Australian Research Council (ARC) Discovery Project DP190102980 to C.T. and J.C.P., National Health and Medical Research Council (NHMRC)

Program grant 1071659, and NHMRC Investigator grant 1174876 to J.C.P., as well as a University of Adelaide Beacon Fellowship to C.T.

The funders had no role in study design, data collection and interpretation, or the decision to submit the work for publication.

## REFERENCES

2010. Nuorti JP, Whitney CG. Prevention of pneumococcal disease among infants and children: use of 13-valent pneumococcal conjugate vaccine and 23-valent pneumococcal polysaccharide vaccine: recommendations of the Advisory Committee on Immunization Practices (ACIP). *MMWR Recomm Rep* 59:1–18. <https://www.cdc.gov/mmwr/preview/mmwrhtml/rr5911a1.htm>.
- Thigpen MC, Whitney CG, Messonnier NE, Zell ER, Lynfield R, Hadler JL, Harrison LH, Farley MM, Reingold A, Bennett NM, Craig AS, Schaffner W, Thomas A, Lewis MM, Scallan E, Schuchat A, Emerging Infections Programs N. 2011. Bacterial meningitis in the United States, 1998–2007. *N Engl J Med* 364:2016–2025. <https://doi.org/10.1056/NEJMoa1005384>.
- WHO. 2007. Pneumococcal conjugate vaccine for childhood immunization: WHO position paper. *Wkly Epidemiol Rec* 82:93–104.
- Gray BM, Converse GM, III, Dillon HC, Jr. 1980. Epidemiologic studies of *Streptococcus pneumoniae* in infants: acquisition, carriage, and infection during the first 24 months of life. *J Infect Dis* 142:923–933. <https://doi.org/10.1093/infdis/142.6.923>.
- Pezzulo AA, Gutierrez J, Duschner KS, McConnell KS, Taft PJ, Ernst SE, Yahr TL, Rahmouni K, Klesney-Tait J, Stoltz DA, Zabner J. 2011. Glucose depletion in the airway surface liquid is essential for sterility of the airways. *PLoS One* 6:e16166. <https://doi.org/10.1371/journal.pone.0016166>.
- Paixao L, Oliveira J, Verissimo A, Vinga S, Lourenco EC, Ventura MR, Kjos M, Veening JW, Fernandes VE, Andrew PW, Yesilkaya H, Neves AR. 2015. Host glycan sugar-specific pathways in *Streptococcus pneumoniae*: galactose as a key sugar in colonisation and infection [corrected]. *PLoS One* 10:e0121042. <https://doi.org/10.1371/journal.pone.0121042>.
- Trappetti C, McAllister LJ, Chen A, Wang H, Paton AW, Oggioni MR, McDevitt CA, Paton JC. 2017. Autoinducer 2 signaling via the phosphotransferase FruA drives galactose utilization by *Streptococcus pneumoniae*, resulting in hypervirulence. *mBio* 8:e02269-16. <https://doi.org/10.1128/mBio.02269-16>.
- Bidossi A, Mulas L, Decorosi F, Colomba L, Ricci S, Pozzi G, Deutscher J, Viti C, Oggioni MR. 2012. A functional genomics approach to establish the complement of carbohydrate transporters in *Streptococcus pneumoniae*. *PLoS One* 7:e33320. <https://doi.org/10.1371/journal.pone.0033320>.
- Afzal M, Shafeeq S, Kuipers OP. 2014. LacR is a repressor of *lacABCD* and LacT is an activator of *lacTFEG*, constituting the *lac* gene cluster in *Streptococcus pneumoniae*. *Appl Environ Microbiol* 80:5349–5358. <https://doi.org/10.1128/AEM.01370-14>.
- Zeng L, Das S, Burne RA. 2010. Utilization of lactose and galactose by *Streptococcus mutans*: transport, toxicity, and carbon catabolite repression. *J Bacteriol* 192:2434–2444. <https://doi.org/10.1128/JB.01624-09>.
- Sun X, Ge F, Xiao CL, Yin XF, Ge R, Zhang LH, He QY. 2010. Phosphoproteomic analysis reveals the multiple roles of phosphorylation in pathogenic bacterium *Streptococcus pneumoniae*. *J Proteome Res* 9:275–282. <https://doi.org/10.1021/pr900612v>.
- Huffman JL, Lu F, Zalkin H, Brennan RG. 2002. Role of residue 147 in the gene regulatory function of the *Escherichia coli* purine repressor. *Biochemistry* 41:511–520. <https://doi.org/10.1021/bi0156660>.
- Fleming E, Lazinski DW, Camilli A. 2015. Carbon catabolite repression by seryl phosphorylated HPr is essential to *Streptococcus pneumoniae* in carbohydrate-rich environments. *Mol Microbiol* 97:360–380. <https://doi.org/10.1111/mmi.13033>.
- Afzal M, Shafeeq S, Manzoor I, Kuipers OP. 2015. GalR Acts as a transcriptional activator of *galKT* in the presence of galactose in *Streptococcus pneumoniae*. *J Mol Microbiol Biotechnol* 25:363–371. <https://doi.org/10.1159/000439429>.
- Echenique J, Kadioglu A, Romao S, Andrew PW, Trombe MC. 2004. Protein serine/threonine kinase StkP positively controls virulence and competence in *Streptococcus pneumoniae*. *Infect Immun* 72:2434–2437. <https://doi.org/10.1128/iai.72.4.2434-2437.2004>.
- Novakova L, Saskova L, Pallova P, Janecek J, Novotna J, Ulrych A, Echenique J, Trombe MC, Branny P. 2005. Characterization of a eukaryotic type serine/threonine protein kinase and protein phosphatase of *Streptococcus pneumoniae* and identification of kinase substrates. *FEBS J* 272:1243–1254. <https://doi.org/10.1111/j.1742-4658.2005.04560.x>.
- Hirschfeld C, Gómez-Mejía A, Bartel J, Hentschker C, Rohde M, Maaß S, Hammerschmidt S, Becher D. 2019. Proteomic investigation uncovers potential targets and target sites of pneumococcal serine-threonine kinase StkP and phosphatase PhpP. *Front Microbiol* 10:3101. <https://doi.org/10.3389/fmicb.2019.03101>.
- Biasini M, Bienert S, Waterhouse A, Arnold K, Studer G, Schmidt T, Kiefer F, Gallo Cassarino T, Bertoni M, Bordoli L, Schwede T. 2014. SWISS-MODEL: modelling protein tertiary and quaternary structure using evolutionary information. *Nucleic Acids Res* 42:W252–W258. <https://doi.org/10.1093/nar/gku340>.
- Lu S, Wang J, Chitsaz F, Derbyshire MK, Geer RC, Gonzales NR, Gwadz M, Hurwitz DI, Marchler GH, Song JS, Thanki N, Yamashita RA, Yang M, Zhang D, Zheng C, Lanczycki CJ, Marchler-Bauer A. 2020. CDD/SPARCLE: the conserved domain database in 2020. *Nucleic Acids Res* 48:D265–D268. <https://doi.org/10.1093/nar/gkz991>.
- Minhas V, Harvey RM, McAllister LJ, Seemann T, Syme AE, Baines SL, Paton JC, Trappetti C. 2019. Capacity to utilize raffinose dictates pneumococcal disease phenotype. *mBio* 10:e02596-18. <https://doi.org/10.1128/mBio.02596-18>.
- Iannelli F, Pozzi G. 2004. Method for introducing specific and unmarked mutations into the chromosome of *Streptococcus pneumoniae*. *Mol Biotechnol* 26:81–86. <https://doi.org/10.1385/MB:26:1:81>.
- Sung CK, Li H, Claverys JP, Morrison DA. 2001. An *rpsL* cassette, Janus, for gene replacement through negative selection in *Streptococcus pneumoniae*. *Appl Environ Microbiol* 67:5190–5196. <https://doi.org/10.1128/AEM.67.11.5190-5196.2001>.
- Livak KJ, Schmittgen TD. 2001. Analysis of relative gene expression data using real-time quantitative PCR and the 2<sup>(-ΔΔC(T))</sup> method. *Methods* 25:402–408. <https://doi.org/10.1006/meth.2001.1262>.
- Tikhomirova A, Trappetti C, Standish AJ, Zhou Y, Breen J, Pederson S, Zilm PS, Paton JC, Kidd SP. 2018. Specific growth conditions induce a *Streptococcus pneumoniae* non-mucoidal, small colony variant and determine the outcome of its co-culture with *Haemophilus influenzae*. *Pathog Dis* 76:fty074. <https://doi.org/10.1093/femspd/fty074>.